Title

Obstructive Sleep Apnea-induced Endothelial Dysfunction Is Mediated by miR-210.

Journal

American Journal of Respiratory and Critical Care Medicine, 207(3)

ISSN

1073-449X

Authors

Shang, Fenqing
Wang, Shen-Chih
Gongol, Brendoan
et al.

Publication Date

2023-02-01

DOI

10.1164/rccm.202202-0394oc

Peer reviewed

ORIGINAL ARTICLE

Obstructive Sleep Apnea–induced Endothelial Dysfunction Is Mediated by miR-210

Fenqing Shang[1,2*], Shen-Chih Wang[3,4*], Brendoan Gongol[5*], So Yun Han[5], Yoshitake Cho[5], Cara R. Schiavon[6], Lili Chen[2], Yuanming Xing[2], Yingshuai Zhao[7], Ming'an Ning[8], Xuan Guo[8], Fangzhou He[2], Yuyang Lei[2], Liuyi Wang[7], Uri Manor[6], Traci Marin[5,9], Kun-Ta Chou[4,10], Ming He[5], Po-Hsun Huang[11,12], John Y.-J. Shyy[5], and Atul Malhotra[13]

[1]Translational Medicine Centre, Xi'an Chest Hospital, and [2]Cardiovascular Research Center, School of Basic Medical Sciences, Xi'an Jiaotong University Health Science Center, Xi'an, China; [3]Department of Anesthesiology, [10]Center of Sleep Medicine, and [12]Department of Critical Care Medicine, Taipei Veterans General Hospital, Taipei, Taiwan; [4]School of Medicine and [11]Cardiovascular Research Center, National Yang Ming Chiao Tung University, Taipei, Taiwan; [5]Division of Cardiology and [13]Division of Pulmonary and Critical Care Medicine, Department of Medicine, University of California, San Diego, La Jolla, California; [6]Waitt Advanced Biophotonics Center, Molecular and Cellular Biology Laboratory, Salk Institute for Biological Studies, La Jolla, California; [7]Department of General Medicine, Henan Provincial People's Hospital, People's Hospital of Zhengzhou University, Zhengzhou, China; [8]Department of Cardiology, Xi'an No. 1 Hospital, Xi'an, China; and [9]Department of Respiratory Therapy, Victor Valley College, Victorville, California

ORCID IDs: 0000-0002-4822-5474 (K.-T.C.); 0000-0002-5625-753X (J.Y.-J.S.).

Abstract

Rationale: Obstructive sleep apnea (OSA)–induced endothelial cell (EC) dysfunction contributes to OSA-related cardiovascular sequelae. The mechanistic basis of endothelial impairment by OSA is unclear.

Objectives: The goals of this study were to identify the mechanism of OSA-induced EC dysfunction and explore the potential therapies for OSA-accelerated cardiovascular disease.

Methods: The experimental methods include data mining, bioinformatics, EC functional analyses, OSA mouse models, and assessment of OSA human subjects.

Measurements and Main Results: Using mined microRNA sequencing data, we found that microRNA 210 (miR-210) conferred the greatest induction by intermittent hypoxia in ECs. Consistently, the serum concentration of miR-210 was higher in individuals with OSA from two independent cohorts. Importantly, miR-210 concentration was positively correlated with the apnea–hypopnea index. RNA sequencing data collected from ECs transfected with miR-210 or treated with OSA serum showed a set of genes commonly altered by miR-210 and OSA serum, which are largely involved in mitochondrion-related pathways. ECs transfected with miR-210 or treated with OSA serum showed reduced $\dot{V}_{O_2}$ rate, mitochondrial membrane potential, and DNA abundance. Mechanistically, intermittent hypoxia-induced SREBP2 (sterol regulatory element–binding protein 2) bound to the promoter region of miR-210, which in turn inhibited the iron–sulfur cluster assembly enzyme and led to mitochondrial dysfunction. Moreover, the SREBP2 inhibitor betulin alleviated intermittent hypoxia–increased systolic blood pressure in the OSA mouse model.

Conclusions: These results identify an axis involving SREBP2, miR-210, and mitochondrial dysfunction, representing a new mechanistic link between OSA and EC dysfunction that may have important implications for treating and preventing OSA-related cardiovascular sequelae.

Keywords: obstructive sleep apnea; endothelium; miR-210; mitochondrial dysfunction

(Received in original form February 23, 2022; accepted in final form October 3, 2022)

*These authors contributed equally to this work.

Supported by NIH grants R01HL148436, HL154926 (A.M.), R01HL106579 (J.Y.-J.S.), F32GM137580 (C.R.S.), and R21DC018237 (U.M.); National Natural Science Foundation of China grant 81800397 (F.S.); and Taipei Veterans General Hospital grant V106C-045 (P.-H.H.). The Waitt Advanced Biophotonics Center was funded by the Waitt Foundation and Core Grant application National Cancer Institute Cancer Center Support Grant CA014195.

Author Contributions: F.S., S.-C.W., B.G., T.M., J.Y.-J.S., and A.M. conceived the original idea and designed the overall experimental plan. F.S., S.-C.W., B.G., S.Y.H., Y.C., C.R.S., L.C., Y.Z., M.N., X.G., F.H., K.-T.C., and Y.L. performed experiments. F.S., S.-C.W., B.G., Y.X., T.M., and M.H. interpreted the data and performed statistical analysis. L.W., U.M., P.-H.H., J.Y.-J.S., and A.M. provided essential input to the overall research plan. F.S., S.-C.W., B.G., M.H., J.Y.-J.S., and A.M. wrote the manuscript. All authors gave final approval of the version to be submitted.

Am J Respir Crit Care Med Vol 207, Iss 3, pp 323–335, Feb 1, 2023

Originally Published in Press as DOI: 10.1164/rccm.202202-0394OC on October 3, 2022
Internet address: www.atsjournals.org

At a Glance Commentary

Scientific Knowledge on the Subject: The serum concentration of microRNA 210 (miR-210) is higher in individuals with obstructive sleep apnea (OSA). Intermittent hypoxia induces miR-210 in cultured vascular endothelial cells via SREBP2 (sterol regulatory element–binding protein 2). The induced miR-210 in turn inhibits the iron–sulfur cluster assembly enzyme, leading to mitochondrial dysfunction in the endothelium.

What This Study Adds to the Field: We describe a novel mechanism by which OSA induces endothelial dysfunction and a new OSA therapeutic potential by inhibiting miR-210 or SREBP2.

Obstructive sleep apnea (OSA) is characterized by repeated pharyngeal collapse during sleep, which leads to hypoxemia, hypercapnia, and catecholamine surges (1–4). Clinically, the severity of OSA is often defined by the apnea–hypopnea index (AHI) (5). The development of cardiovascular diseases including systemic hypertension, metabolic syndrome, and atherosclerosis is often accelerated by OSA (6–8). Vascular endothelial cells (ECs) lining the luminal surface of the vasculature are in direct contact with the circulating paracrine, autocrine, and hormonal mediators. During OSA onset, ECs are exposed to multiple factors that are enhanced in the circulation, including periods of cycling hypoxia, dysregulated metabolic factors, and inflammation (9–12). Collectively, these detrimental factors aggravate EC dysfunction by impairing mitochondrial function, increasing reactive oxygen species production, and reducing nitric oxide (NO) bioavailability (13).

MicroRNAs (miRNAs) are important regulators of cellular functions by targeting mRNAs complementary to their seed sequence, which results in reduced gene expression (14). Several miRNAs (miRNAs) have been implicated in OSA pathophysiology, including miR-664a-3p, miR-92a, and miR-1254 (15–17). Despite the propensity of vascular dysfunction in individuals with OSA, a comprehensive understanding of the miRNAs involved in EC biology in response to OSA is lacking.

As a hypoxia-induced miRNA (18, 19), miR-210 is an important regulator of cell function via its downregulation of mitochondrial biogenesis, which attenuates oxidative phosphorylation demand (20–22). Because ECs have little capacity for energy storage, endothelium relies on mitochondrial biochemical changes to maintain energy demand and homeostasis. As such, in homeostatic ECs, functional mitochondria facilitate ATP production and enhance NO bioavailability (23). The dynamic changes in mitochondrial biogenesis, including the mitochondrial iron–sulfur cluster (ISC), determine EC homeostasis or dysfunction (24, 25). The ISC assembly enzyme (ISCU) regulates the assembly of the ISC in mitochondria and thus is pivotal for the electron transporter chain in complexes I, II, and III activity and fatty acid oxidation (26, 27). A dysregulated ISCU renders mitochondrial dysfunction by impairing oxidative phosphorylation (28). Of note, ISCU is a bona fide target of miR-210 by targeting the ISCU mRNA 3′ untranslated region (24, 27). The hypoxia-induced miR-210–ISCU axis leading to dysfunctional ECs is manifested in patients with pulmonary hypertension and in rodent pulmonary hypertension models (29). In the lung endothelium of such mouse models, miR-210 induced by HIF1α (hypoxia-inducible factor 1-α) decreased ISCU, ISC biogenesis, and consequent mitochondrial respiration.

SREBP1 (sterol regulatory element–binding protein 1) and SREBP2 are key transcription factors regulating genes involved in triglyceride and cholesterol biosynthesis (30). Besides their canonical role in lipid metabolism, SREBP1 and SREBP2 are involved in innate immune responses in several cell types, including monocytes, macrophages and ECs (31–33). Activation of SREBPR2 in ECs activates NLRP3 (NOD-like receptor family pyrin domain–containing protein 3), with consequent induction of NLRP3 inflammasome and IL-1β–family proteins (31). In addition, SREBP2 activates miR-92a, which targets Kruppel-like factors 2 and 4, two master transcription factors in ECs (32). In essence, SREBP2 activation promotes the innate immune response and EC dysfunction.

In this study, *in vitro* and *in vivo* OSA models were used to show that EC dysfunction was associated with the occurrence of OSA. The underlying mechanism involved SREBP2 induction of miR-210 in ECs, leading to ISCU downregulation, mitochondrial impairment, and metabolic shunt (i.e., increased glycolysis). Clinical data from two groups of subjects with OSA indicated that serum concentration of miR-210 was positively associated with the AHI. These new mechanistic insights provide a novel therapeutic target to mitigate OSA-induced vascular risk.

Methods

Additional detail on the methods for making these measurements is provided in the online supplement.

Patients

We conducted our studies in compliance with recognized international standards, including the principles of the Declaration of Helsinki. The study was approved by respective local institutional review boards, and all participants provided informed consent. Patients with different severity of OSA syndrome and age- and sex-matched OSA-free individuals were recruited from Xi'an No. 1 Hospital in Xi'an, China (cohort 1), and Taipei Veterans General Hospital in Taipei, Taiwan (cohort 2), from 2017 to 2019. The blood samples were obtained in unheparinized Vacutainers (Becton Dickinson), and clots were removed by centrifuging at 3,000 rpm for 15 minutes. Supernatants were collected for analyses of serum creatinine and miR-210 concentrations. The demographic and

Correspondence and requests for reprints should be addressed to John Y.-J. Shyy, Ph.D., Division of Cardiology, Department of Medicine, University of California, San Diego, 9500 Gilman Drive, La Jolla, CA 92093. E-mail: jshyy@health.ucsd.edu.

This article has a related editorial.

This article has an online supplement, which is accessible from this issue's table of contents at www.atsjournals.org.

clinical characteristics of study participants are provided in Tables 1 and 2.

Clinical Data Analytics

Analysis of clinical data involved using R (https://www.r-project.org/) supported by data.table (https://github.com/Rdatatable/data.table) packages. miR fold changes were computed using the $-\Delta\Delta$ct method (34), and between-site variability was normalized to the average of the control group for each site. Resulting fold changes were then $\log_2$ normalized, and tests of normality involved using a Shapiro-Wilk test. We used multivariable logistic regression analysis and correlation analysis with nonparametric Spearman correlations.

Intermittent Hypoxia Mouse Model

Institutional Animal Care and Use Committee approval was obtained from Taipei Veterans General Hospital (2019-097), and experiments were performed on male, age-matched C57BL/6J mice (8–12 weeks old) provided by the National Laboratory Animal Center of Taiwan. Severe OSA (AHI = 40) was simulated by exposing mice to intermittent hypoxia (IH) consisting of 60 seconds of 21% O_2 followed by 30 seconds of 10% O_2 cycles for 8 h/d with the OxyCycler A84 (BioSpherix). After 2-week exposure, mice were killed, and blood, lung, and aortic tissue samples were collected. In total, 40 mice were randomly assigned to control and IH groups. Betulinic acid (B8936; Sigma-Aldrich) was administered by daily oral gastric feeding starting 1 week before IH exposure with 200 μl of 20 mg/kg betulinic acid solution dissolved in 3% DMSO. The creation of the EC-SREBP2(N)-Tg mouse model was described previously (31).

Statistical Analysis

All results are presented as mean ± SEM. Initially, data were tested for normality and equal variance to confirm the appropriateness of parametric tests. Experiments with two groups were compared using a two-tailed Student's *t* test for parametric data or the Mann-Whitney *U* test for nonparametric data or data with sample size ⩽ 6. Experiments with more than two groups were compared using one-way ANOVA with a Bonferroni *post hoc* test for parametric data or the Kruskal-Wallis test with Dunn's multiple comparisons for nonparametric data or data with sample size ⩽ 6. All statistical analyses involved using GraphPad Prism 5.01. A two-tailed *P* value <0.05 was considered to indicate statistical significance.

Table 1. Characteristics of Control Subjects and Participants with Obstructive Sleep Apnea in Cohort 1

	Control Group	OSA Group	*P* Value
Number	16	46	—
Sex (male/female), *n*	10/7	41/6	0.0775
Age, yr	45.5 ± 14.1	47.22 ± 12.6	0.4939
Height, cm	167.69 ± 7.22	169.98 ± 8.06	0.1514
Weight, kg	75.75 ± 11.41	85.12 ± 12.35	**0.0315**
BMI, kg/m^2	26.7 ± 3.57	29.3 ± 4.69	0.0881
Hypertension, *n*	4	24	0.1119
Coronary heart disease, *n*	0	1	1.0000
SBP, mm Hg	137.25 ± 22.03	145.75 ± 22.94	0.1185
DBP, mm Hg	84.75 ± 12.7	88.36 ± 19.18	0.4688
hs-CRP, mg/L	0.71 ± 0.24	2.42 ± 1.56	**0.0001**
TC, mmol/L	4.03 ± 1.16	4.43 ± 1.15	0.0996
TG, mmol/L	1.55 ± 1.07	2.31 ± 1.44	**0.0291**
HDL-C, mmol/L	1.17 ± 0.43	1.08 ± 0.21	0.6820
LDL-C, mmol/L	2.26 ± 0.93	2.77 ± 0.86	0.0882
Glucose, mmol/L	5.07 ± 1.15	5.0 ± 0.82	0.8218
ALT, U/L	21.27 ± 8.53	23.02 ± 7.83	0.7807
AST, U/L	22.88 ± 10.65	28.75 ± 18.83	0.9647
BUN, mmol/L	5.05 ± 1.93	5.25 ± 1.25	0.8281
Creatinine, μmol/L	73.21 ± 24.09	80.94 ± 15.02	0.2307
AHI	2.24 ± 0.95	31.23 ± 22.52	**0.0000**
ODI	4.24 ± 3.85	28.22 ± 22.02	**0.0000**
Sa_{O_2} nadir (sleep), %	86.25 ± 3.98	74.39 ± 11.75	**0.0000**
Insulin, μIU/ml	8.76 ± 6.20	17.30 ± 17.34	**0.0148**

Definition of abbreviations: AHI = apnea–hypopnea index; ALT = alanine aminotransferase; AST = alanine aminotransferase; BMI = body mass index; BUN = blood urea nitrogen; DBP = diastolic blood pressure; HDL-C = high-density lipoprotein cholesterol; hs-CRP = high sensitivity C-reactive protein; LDL-C = low-density lipoprotein cholesterol; ODI = oxygen desaturation index; OSA = obstructive sleep apnea; SBP = systolic blood pressure; TC = total cholesterol; TG = triglycerides.
Data are expressed as mean ± SD unless otherwise indicated. *P* values in boldface type denote statistical significance.

Results

Hypoxia Induces miR-210 in ECs

To comprehend the involvement of miRNA in OSA-associated EC dysfunction, we first mined miRNA sequencing data (Gene Expression Omnibus: GSE116909) (35) generated from human umbilical vein ECs (HUVECs) exposed to sustained hypoxia for 3.2, 8, or 14.2 hours or IH (two, five, or nine cycles of 1 h hypoxia [0.9% O_2] followed by 36 min normoxia [21% O_2]) or cultured under normoxia as a control (Figure 1A). Among hypoxia-induced miRNAs with fold change >1 with $P<0.05$, miR-210 exhibited the greatest cycle- and time-dependent response compared with the normoxic control (Figure 1B; *see* Table E1 in the online supplement). Using cultured HUVECs under sustained hypoxia (e.g., 1% O_2) for various durations (Figure 1C) or IH for up to nine cycles (Figure 1D), we validated the hypoxia induction of miR-210. As anticipated, hypoxia induced miR-210 in ECs in a time- and cycle-dependent manner (Figures 1C and 1D).

Elevated Concentration of miR-210 in the OSA Serum

Given that hypoxia increases the circulatory concentration of miR-210 in mice (36), we then asked whether miR-210 concentration is elevated in the circulation of patients with OSA. Data collected from two independent cohorts (demographic and clinical characteristics of study participants are provided in Tables 1 and 2) showed that serum concentrations of miR-210 were higher in individuals with OSA than in healthy control subjects (Figure 1E). Significantly, miR-210 concentration was positively correlated with AHI in all participants (Figure 1F), which indicates

Table 2. Characteristics of Control Subjects and Participants with Obstructive Sleep Apnea in Cohort 2

	Control Group	OSA Group	*P* Value
Number	22	19	—
Sex (male/female), *n*	16/6	16/3	0.0995
Age, yr	65.1 ± 8.9	60.0 ± 11.4	0.1360
Height, cm	166.3 ± 8.1	166.5 ± 9.5	1.0000
Weight, kg	67.8 ± 11.4	81.0 ± 19.5	0.1617
BMI, kg/m^2	25.2 ± 3.5	29.0 ± 5.4	**0.0205**
Smoking, *n*	7	10	0.6112
Hypertension, *n*	8	16	**0.0287**
Diabetes mellitus, *n*	5	9	0.3740
Oral hypoglycemic agent, *n*	5	7	0.8124
Stroke, *n*	1	0	0.9781
Chronic kidney disease, *n*	2	1	0.9610
SBP, mm Hg	118.8 ± 12.2	124.1 ± 13.6	0.2856
DBP, mm Hg	71.1 ± 9.9	70.7 ± 9.3	0.9711
TC, mmol/L	4.20 ± 1.14	4.25 ± 0.63	0.8001
TG, mmol/L	1.17 ± 0.35	1.54 ± 0.60	**0.0321**
HDL-C, mmol/L	1.17 ± 0.30	1.08 ± 0.27	0.2289
LDL-C, mmol/L	2.65 ± 1.07	2.42 ± 0.60	0.8079
Glucose, mmol/L	5.59 ± 1.23	6.81 ± 2.28	**0.0444**
ALT, U/L	19.75 ± 3.20	27.89 ± 20.17	0.9674
AST, U/L	20.33 ± 2.52	24.53 ± 15.27	0.8732
eGFR, ml/min/1.73 m^2	67.23 ± 17.22	82.23 ± 26.30	0.0616
AHI	2.83 ± 1.90	28.69 ± 25.97	**0.0002**
ODI	2.80 ± 1.94	24.68 ± 21.69	**0.0023**
Sa_{O_2} nadir (sleep), %	89.75 ± 2.50	78.32 ± 9.77	**0.0022**

Definition of abbreviations: AHI = apnea–hypopnea index; ALT = alanine aminotransferase; AST = alanine aminotransferase; BMI = body mass index; BUN = blood urea nitrogen; DBP = diastolic blood pressure; eGFR = estimated glomerular filtration rate; HDL-C = high-density lipoprotein cholesterol; hs-CRP = high sensitivity C-reactive protein; LDL-C = low-density lipoprotein cholesterol; ODI = oxygen desaturation index; OSA = obstructive sleep apnea; SBP = systolic blood pressure; TC = total cholesterol; TG = triglycerides.
Data are expressed as mean ± SD unless otherwise indicated. *P* values in boldface type denote statistical significance.

that serum concentration of miR-210 depended on the severity of sleep apnea. In addition to miR-210, our univariable analyses indicated that body mass index (BMI), AHI, oxygen desaturation index, tst88 (total sleep time with O2 saturation < 88%), and Sa_{O_2} nadir score could also predict OSA pathophysiology (*see* Table E2). However, the ability of miR-210 to predict OSA pathophysiology was not affected by these attributes in multivariable models (*see* Table E3). Of note, the stratification analysis results indicated that miR-210 is still a significant predictor of OSA in both normal-weight (BMI $<$ 25 kg/m^2) and overweight (BMI $\geqslant$ 25 kg/m^2) individuals. Although miR-210 predicted OSA in individuals not taking any medications, the effect of drugs on miR-210 expression could not be controlled for individuals taking medications, because of a limited sample size among these taking medications who did not have OSA. To decipher whether the elevated miR-210 concentrations in patients with OSA originated, at least in part, from vascular endothelium, we analyzed miR-210 concentrations in EC-derived microparticles immunoprecipitated from serum by anti–CD31 (cluster of differentiation 31) antibody. Concentrations of miR-210 were higher in CD31-enriched microparticles from OSA than healthy control serum (Figure 1G). Thus, OSA severity was correlated with the circulatory concentration of miR-210, and vascular endothelium likely contributed to the increased miR-210 concentration. Considering the significant differences in BMI between the control and OSA groups in cohort 2 (25.2 ± 3.5 vs. 29.0 ± 5.4 kg/m^2, respectively; $P = 0.0205$), we then performed multivariable analyses with BMI and miR-210 to test whether BMI can affect the ability of miR-210 to predict OSA. Our analysis indicated that BMI is a copredictor of OSA together with miR-210. Of note, the stratification analysis results indicated that miR-210 is still a significant predictor of OSA in both normal-weight (BMI $<$ 25 kg/m^2) and overweight (BMI $\geqslant$ 25 kg/m^2) individuals.

OSA Impairs Mitochondrial Function via miR-210

To infer how OSA affects EC function via miR-210 elevation, we analyzed RNA sequencing data collected from ECs transfected with miR-210 versus a scramble control as well as ECs treated with OSA versus control serum. ECs overexpressing miR-210 and those treated with OSA serum exhibited 336 and 3,654 differentially expressed genes (DEGs), respectively, compared with respective controls. Among these two sets of DEGs, 101 genes were commonly induced by miR-210 and OSA serum, which accounted for ~30% of the miR-210–induced genes (Figure 2A). Metascape Gene Ontology enrichment analysis indicated that these genes are largely involved in the inflammatory response, mitochondrial respirasome, mitochondrial transcription, IL-17 signaling, TNF (tumor necrosis factor) signaling, response to chemokine, TGF-β (transforming growth factor-β) signaling, regulation of autophagy, and response to hypoxia (Figure 2A). The heatmap in Figure 2B shows that the genes belonging to the three mitochondrion-related pathways (i.e., mitochondrial respirasome, mitochondrial transcription, and mitochondrial membrane organization) were commonly downregulated by miR-210 and OSA serum.

To correlate results from these *in silico* analyses with OSA serum, EC dysfunction, and elevated miR-210 concentration, we observed mitochondrial changes in miR-210–transfected or OSA serum–incubated ECs. Confocal microscopy shown in Figure 3A revealed apparent mitochondrial fragmentation, which indicates altered mitochondrial dynamics by miR-210 and OSA serum. Consistently, ECs treated with OSA serum showed reduced mitochondrial abundance and membrane potential, as revealed by MitoTracker and JC-1 staining (Figures 3B and 3C; *see* Figure E1). This detrimental effect of OSA serum was mitigated in ECs transfected with anti–miR-210. Hypoxia induction of miR-210 has been suggested to alter cellular metabolism by downregulating the mitochondrial electron transport chain, namely, complexes I and III (24). We used $\dot{V}O_2$ rate analysis to test whether OSA serum, like miR-210, induced a

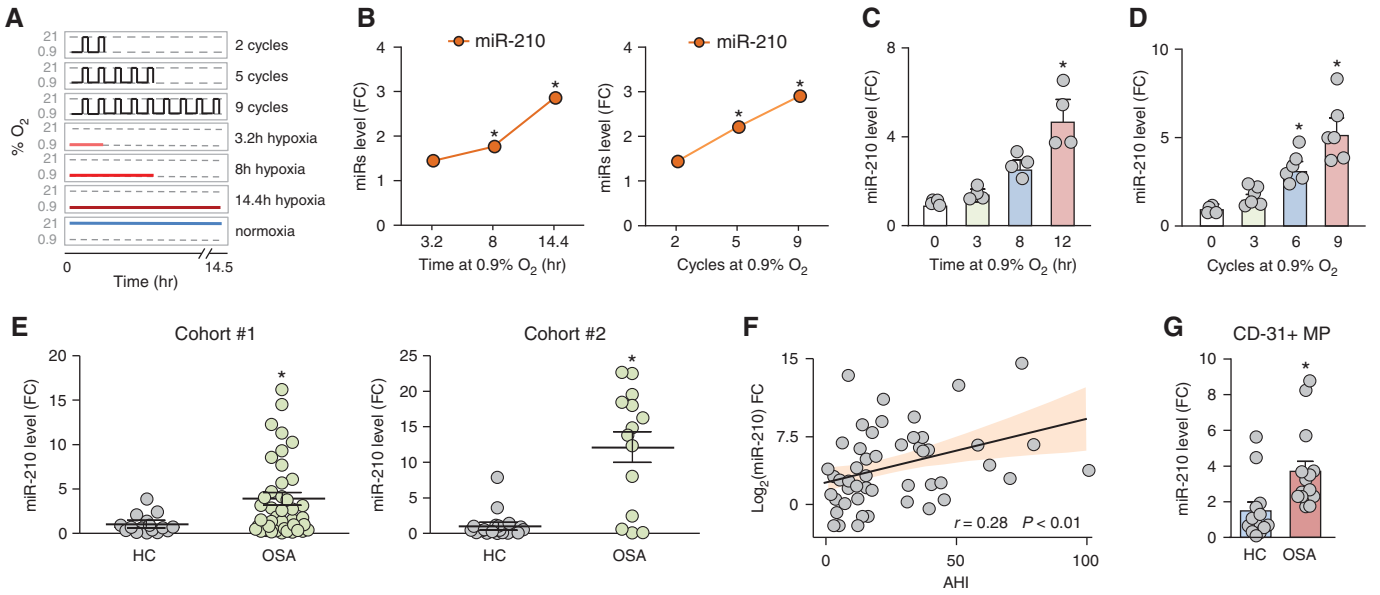

Figure 1. Endothelial cell–derived microRNA 210 (miR-210) is induced in obstructive sleep apnea (OSA). (*A* and *B*) miR expression concentrations were mined from the online data set GSE116909 (Gene Expression Omnibus) (35). This data set was collected from experiments using human umbilical vein endothelial cells (HUVECs) exposed to sustained (0.9% O_2) or intermittent (0.9% O_2 for 1 h and then normoxia for 36 min per cycle) hypoxia for the indicated time or cycle (*A*). Expression of miR-210-3p is highlighted by red dots and lines (*B*). (*C* and *D*) miR-210 expression in HUVECs exposed to sustained or intermittent hypoxia for the indicated time (*C*) or cycles (*D*) detected using quantitative PCR (qPCR); U6 was an internal control. (*E*) Circulating concentration of miR-210 was quantified using qPCR in age- and sex-matched healthy control subjects (HCs; $n = 17$ in cohort 1, $n = 22$ in cohort 2) and individuals with OSA ($n = 47$ in cohort 1, $n = 18$ in cohort 2) in two different cohorts. The apnea–hypopnea index (AHI) was evaluated using the sleep apnea test. (*F*) Pearson correlation analysis of correlation between $\log_2$ FC of miR-210 serum concentration and AHI. (*G*) $CD31^+$ MPs were isolated from serum from patients with OSA ($n = 13$) and age-matched HCs ($n = 14$). The concentration of miR-210 was detected using qPCR; *Caenorhabditis elegans* miR-39 was a spike-in control. Data are shown as mean ± SEM. Statistical significance was determined using a two-tailed *t* test or the Mann-Whitney *U* test. $^*P < 0.05$ compared with control or HCs. FC = fold change; miR = microRNA; MP = microparticles.

detrimental respiratory chain in ECs. ECs treated with OSA serum showed reduced basal mitochondrial respiration, ATP production, maximal respiration, and spare capacity compared with ECs treated with control serum (Figure 3D). Importantly, ECs with miR-210 overexpression showed similar impairment of mitochondrial respiration. Pretreatment of anti–miR-210 in ECs partially restored OSA serum reduced $\dot{V}O_2$ rate (Figure 3D).

OSA-induced miR-210 Targets ISCU

Given that several mitochondrial pathways were commonly affected by OSA and miR-210 (Figure 2), we then examined the expression of genes involved in mitochondrial function, including the miR-210–targeted ISCU. OSA serum greatly inhibited concentrations of ISCU compared with other mitochondrial marker genes (Figures 4A and 4B). As a control, miR-210 overexpression in ECs decreased ISCU expression dose-dependently (Figure 4C), consistent with previous findings from Chan and colleagues (24). Importantly, OSA serum inhibition of ISCU mRNA was rescued in ECs cotreated with the miR-210 inhibitor anti-210 (Figure 4D). Next, we measured mRNA concentrations of miR-210 and ISCU in miRNA-induced silencing complex in the context of OSA reduction of ISCU expression. Indeed, we found enhanced binding of miR-210 and ICSU mRNA to AGO2 immunoprecipitated from ECs treated with OSA serum (Figure 4E). To assess direct ISCU mRNA targeting by miR-210, we constructed the wild-type ISCU luciferase reporter construct or a mutant with the miR-210 binding site had been mutated. OSA serum significantly reduced luciferase activity in ECs transfected with the wild-type ISCU reporter versus the mutant ISCU reporter (Figure 4F). Together, Figures 2, 3, and 4 suggest that OSA-reduced mitochondrial activity in endothelium was due in part to miR-210 targeting ISCU expression.

SREBP2 Regulates the miR-210–ISCU Axis

With the defined miR-210–ISCU targeting involved in OSA-impaired endothelium, we next explored the upstream mechanism by which OSA induces miR-210. To infer transcription factors that are involved in the transactivation of the *miR-210* gene, we first analyzed transcription factor binding sequences located at the promoter regions of the 336 DEGs induced by OSA. SREBP2 binding motif was one of the top-ranked *cis* elements involved in OSA-regulated genes (Figure 5A). In addition, low-density lipoprotein, a well-known activator of TNF-α stimulating SREBP2 (37, 38), may be a clinical marker that correlates with (*see* Table E4) and predicts (*see* Table E5) serum miR-210 concentration. Furthermore, SREBP2 is activated in ECs by inflammatory stimuli (31). Using Encyclopedia of DNA Elements data displaying the assay for transposase-accessible chromatin and H3K27ac (acetylated lysine 27 of histone H3) landscapes in ECs, we first

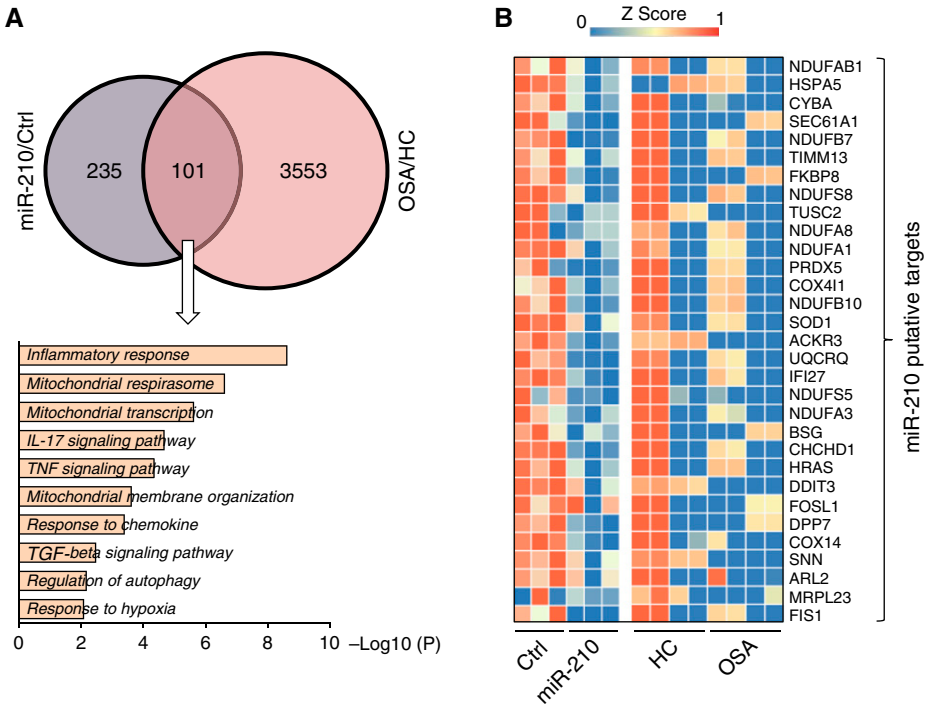

Figure 2. Mitochondrial function impaired by SREBP2 (sterol regulatory element–binding protein 2)–microRNA 210 (miR-210) in endothelial cells (ECs) revealed by RNA sequencing (RNA-seq). (*A*) Human umbilical vein ECs were treated with pooled obstructive sleep apnea (OSA) serum (from three patients with OSA with apnea–hypopnea index > 30) or age- and sex-matched pooled healthy control (HC) serum for 24 hours or transfected with miR-210 or scramble control for 48 hours. RNA was extracted from these cells for RNA-seq. Differentially expressed genes (DEGs [$\log_2$ fold change > 1.5; $P < 0.05$]) were compared between OSA/HC RNA-seq and miR-210/control RNA-seq. We used Metascape Gene Ontology enrichment analysis of the overlapped DEGs from OSA/HC and miR-210/control RNA-seq results plotted as $-\log_{10}(P$ value). (*B*) The heatmap shows the RNA concentrations of mitochondrial function–related genes from OSA/HC and miR-210/control RNA-seq. ACKR3 = atypical chemokine receptor 3; ARL2 = ADP ribosylation factor like GTPase 2; BSG = basigin (Ok blood group); CHCHD1 = coiled-coil-helix-coiled-coil-helix domain containing 1; COX14 = cytochrome C oxidase assembly factor COX14; COX4I1 = cytochrome C oxidase subunit 4I1; Ctrl = control; CYBA = cytochrome B-245 alpha chain; DDIT3 = DNA damage inducible transcript 3; DEG = differentially expressed gene; DPP7 = dipeptidyl peptidase 7; FIS1 = fission, mitochondrial 1; FKBP8 = FKBP prolyl isomerase 8; FOSL1 = FOS like 1, AP-1 transcription factor subunit; HRAS = HRas proto-oncogene, GTPase; HSPA5 = heat shock protein family A (Hsp70) member 5; IFI27 = interferon alpha inducible protein 27; MRPL23 = mitochondrial ribosomal protein L23; NDUF = NADH:ubiquinone oxidoreductase; PRDX5 = peroxiredoxin 5; SEC61A1 = SEC61 translocon subunit alpha 1; SNN = stannin; SOD1 = superoxide dismutase 1; TGF = transforming growth factor; TIMM13 = translocase of inner mitochondrial membrane 13; TNF = tumor necrosis factor; TUSC2 = tumor suppressor 2, mitochondrial calcium regulator; UQCRQ = ubiquinol-cytochrome C reductase complex III subunit VII.

defined the miR-210 promoter region by referencing the assay for transposase-accessible chromatin and H3K27ac peak enrichments (chr11:568626–569682; Figure 5B, highlighted region). Sequence analysis revealed six putative SREBP2 binding motifs in the miR-210 promoter (Figure 5B). Chromatin immunoprecipitation analysis of ECs overexpressing SREBP2 verified the binding of SREBP2 to sites 1 and 3 but not sites 2, 4, 5, and 6 (Figure 5B). Cultured ECs treated with OSA serum showed increased expression of SREBP2 (Figure 5C). *In vivo*, miR-210 concentration was elevated in lung tissue and serum isolated from EC-specific SREBP2-overexpression transgenic mice (EC-SREBP2-Tg; Figure 5D). *In vitro*, OSA serum–induced miR-210 concentration in ECs was attenuated by SREBP2 knockdown or botulin treatment, an SREBP2-inhibitory triterpene (Figures 5E and 5F). Collectively, these data suggest that SREBP2 is a key transcription factor governing miR-210 expression in ECs by OSA.

With SREBP2 transactivating miR-210 in ECs, we then explored the role of SREBP2 in OSA serum–decreased ISCU. As anticipated, OSA serum inhibition of ISCU in cultured ECs was attenuated by SREBP2 siRNA (Figure 6A) or betulin (Figure 6B). *In vivo*, mouse ISCU mRNA concentration was attenuated in aortas of EC-SREBP2-Tg mice compared with wild-type littermates (Figure 6C). ISCU plays an essential role in regulating cellular iron homeostasis and electron transport in the mitochondrial respiratory chain (26). In line with this notion, OSA serum attenuation of mitochondrial respiratory complex I activity in ECs was partially rescued by SREBP2 siRNA or betulin treatment (Figure 6D). Furthermore, mitochondrial DNA content and complex I activity were reduced in aortas of EC-SREBP2-Tg mice compared with wild-type littermates (Figure 6E; *see* Figure E2).

SREBP2–miR-210-ISCU Axis in Mouse OSA Models

With translational implications in mind, we validated the SREBP2–miR-210–ISCU axis in an OSA mouse model. To that end, C57Bl/6j mice were challenged with 2 weeks of IH to mimic the pathophysiological process of OSA. Compared with control

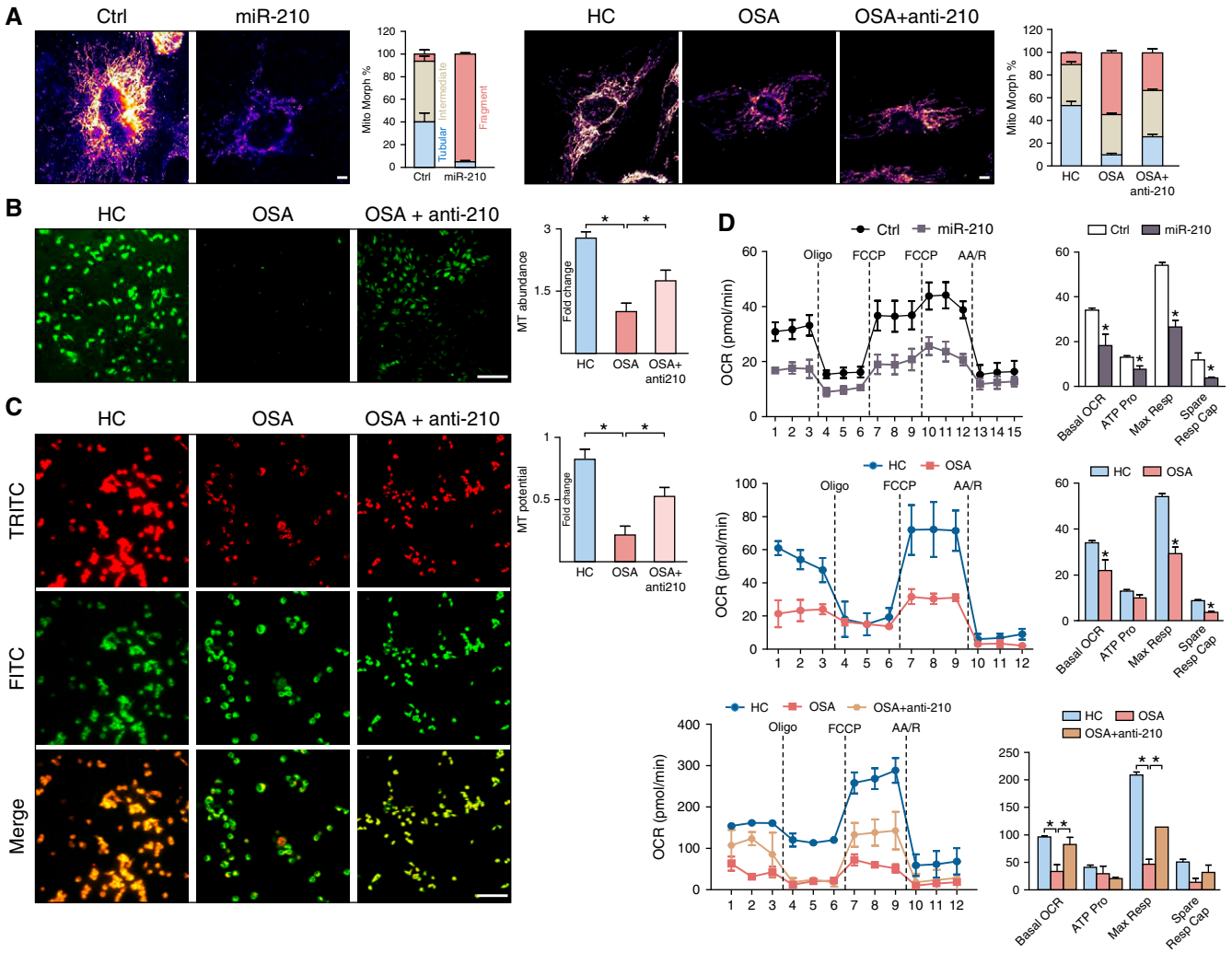

Figure 3. Obstructive sleep apnea (OSA) serum–induced microRNA 210 (miR-210) impairs mitochondrial function in endothelial cells (ECs). (*A–D*) Human umbilical vein ECs were transfected with pro–miR-210 or scramble Ctrl for 48 hours (*A* and *D*) or transfected with anti–miR-210 for 24 hours, followed by incubation of pooled OSA or healthy control (HC) serum for another 24 hours (*A–D*). In *A*, representative confocal images of mitochondrial morphology are shown. Mitochondria were visualized by using TOM20 antibody (50 cells counted for each replicate). Scale bar, 2.5 μm. Tubular: most mitochondria in ECs were >10 μm long; intermediate: mitochondria were <≈10 μm; fragment: most mitochondria were spherical (no clear length or width). In *B*, mitochondrial abundance was assessed using MT. In *C*, mitochondrial membrane potential was detected using JC-1 staining. In *B* and *C*, scale bar, 200 μm. In *D*, the OCR was detected using Seahorse (https://www.agilent.com/en/promotions/seahorse-xf-hs-mini-analyzer?gclid=Cj0KCQiAmaibBhCAARIsAKUlaKRfws3HpgQdtLNaDZzm9zOaQ6XoyUJTszxz-VYXPn6NArHA5PqxBPwaArPxEALw_wcB&gclsrc=aw.ds) assay. Data are shown as mean ± SEM. Statistical significance was determined using one-way ANOVA followed by Bonferroni *post hoc* test or two-tailed Student's *t* test. $^*P < 0.05$ compared with Ctrl or HC or between indicated two groups. AA/R = antimycin A and rotenone; Ctrl = control; FCCP = carbonyl cyanide-4 (trifluoromethoxy) phenylhydrazone; FITC = fluorescein isothiocyanate; Max Resp = maximal respiration; MT = MitoTracker; OCR = $\dot{V}O_2$ rate; Pro = production; Resp Cap = respiratory capacity; TRITC = tetramethylrhodamine.

animals, mice under IH showed significantly decreased body weight (25.18 vs. 29.55 g) and elevated blood pressure (117/68 vs. 99/59 mm Hg) (Figure 7A). This phenotype is consistent with a previous report of the effects of IH on mouse vital signs (39). The concentration of miR-210 was increased and the concentration of $CD31^+$ microparticle-associated miR-210 was elevated in serum from IH mice (Figures 7B and 7C), which suggests that elevated miR-210 concentration is related to vascular endothelium. To investigate ISCU1/2 concentration and mitochondrial function impaired by the SREBP2–miR-210 axis in ECs, we investigated mRNA and protein concentrations from the aortic intima of these mice. Both mRNA and protein concentrations of SREBP2 were increased and ISCU1/2 concentrations were decreased in the IH mouse aortic intima (Figures 7D and 7E). As a functional readout, we detected lower mitochondrial respiratory complex I activity in lung ECs from IH mice (Figure 7F). Furthermore, betulin administration alleviated IH-increased systolic blood pressure (Figure 7G), decreased SREBP2 concentration, and rescued ISCU1/2 concentration (Figure 7H).

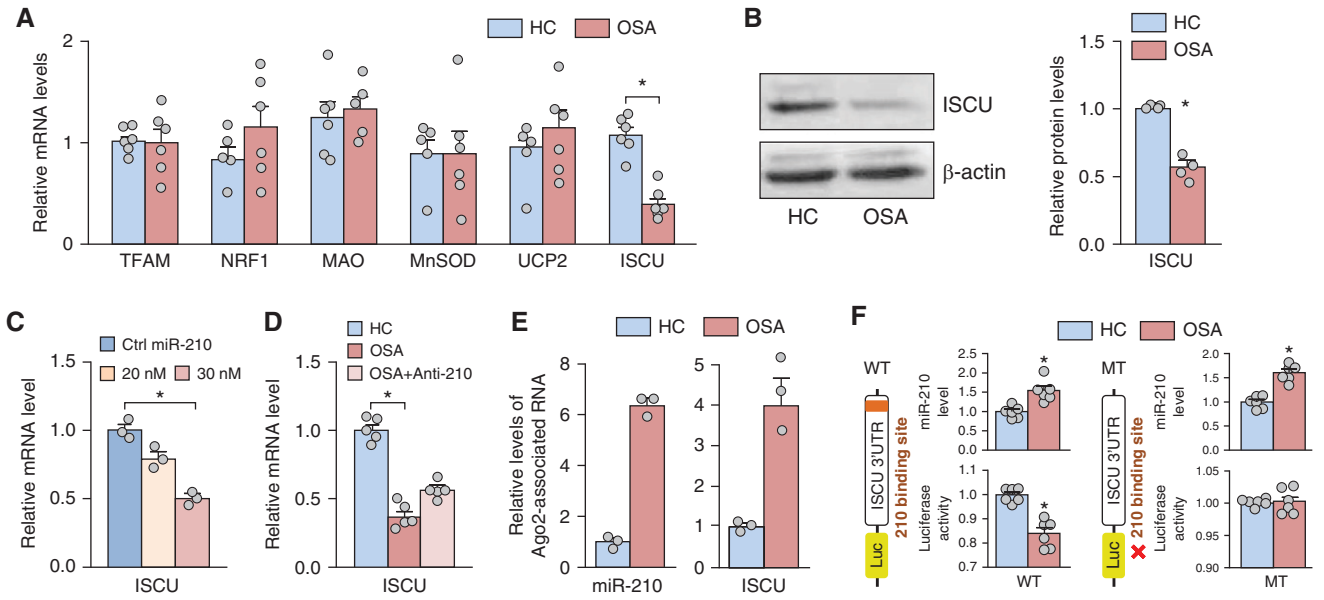

Figure 4. Obstructive sleep apnea (OSA) serum–induced miR-210 inhibits iron–sulfur cluster assembly enzyme (ISCU) in ECs. (*A* and *B*) Human umbilical vein endothelial cells (HUVECs) were treated with 10% pooled OSA or healthy control (HC) serum for 24 hours. The mRNA concentrations of indicated genes (*A*) or ISCU protein (*B*) were detected using quantitative PCR (qPCR) or western blot analysis, respectively. β-Actin was used as an internal control. (*C* and *D*) HUVECs were transfected with 20 or 30 nM microRNA 210 (miR-210) (*C*) or with anti–miR-210 combined with OSA or HC serum (*D*). ISCU mRNA concentration was detected using qPCR. (*E*) HUVECs were treated with pooled OSA or HC serum for 48 hours, followed by Ago2 (argonaute RISC catalytic component 2) RNA immunoprecipitation. Ago2-associated miR-210 and ISCU mRNA concentrations were quantified using qPCR. (*F*) Bovine aorta ECs were transfected with Luc-ISCU-3′UTR (WT) or Luc-ISCU-3′UTR (MT) for 24 hours, then pooled OSA or HC serum for another 24 hours. Luc activity was measured with Renilla as transfection control. miR-210 was quantified using qPCR. Data are shown as mean ± SEM from at least three independent experiments. Statistical significance was determined using the Kruskal-Wallis test with Dunn's multiple comparisons or the two-tailed Mann-Whitney *U* test. $^*P < 0.05$ compared with control, HC, or indicated groups. Ctrl = control; EC = endothelial cell; Luc = luciferase; MAO = monoamine oxidase; MnSOD = manganese superoxide dismutase; MT = miR-210 targeting site TCCCTCT replaced by ACGCACA; NRF1 = nuclear respiratory factor 1; TFAM = transcription factor A, mitochondrial; UCP2 = uncoupling protein 2; UTR = untranslated region; WT = wild-type.

Discussion

This study, encompassing clinical, *in vitro*, and animal experiments, revealed the molecular mechanisms by which OSA causes EC dysfunction. The new findings are as follows: *1*) miR-210 concentration was higher in patients with OSA than in matched control subjects; *2*) the AHI was positively correlated with miR-210 concentration among individuals with OSA, thus suggesting a critical role of miR-210 in OSA pathophysiology; *3*) ECs treated with serum from OSA individuals or transfected with miR-210 showed mitochondrial dysfunction; *4*) OSA-induced SREBP2 transactivated miR-210; and *5*) the SREBP2–miR-210–ISCU axis was induced in an OSA mouse model. These results establish an OSA-induced SREBP2–miR-210 axis in the vascular endothelium that could be a culprit underlying various cardiovascular sequelae.

Autonomic, oxidative stress, inflammatory, and hemostatic abnormalities may be associated with OSA pathogenesis (40–42). However, less is known about the molecular basis underlying OSA-provoked vascular impairment. Our salient finding herein is that OSA-induced miR-210 is causative of EC mitochondrial dysfunction by targeting genes involved in ISC biogenesis. Because ISCU is essential for cellular iron homeostasis, contributing to electron transfer in complexes I, II, and III and redox balance (26, 43), miR-210 targeting ISCU could play a major role in impaired mitochondrial biogenesis and function in vascular endothelium in the context of OSA.

Results in Figure 5D demonstrate that miR-210 concentrations were increased in lung tissues. Although evidence is lacking on whether and how OSA induces miR-210 in pulmonary endothelium, it is conceivable that the OSA-associated hypoxia might be causative for miR-210 induction in the lung. If so, this situation is reminiscent of miR-210 significantly upregulated under hypoxia in a wide range of cell types, including ECs, fibroblasts, and various cancer cells (24, 44, 45). As such, OSA models using inspired hypoxic mixtures likely contribute to hypoxia in the lung tissue, whereas OSA *in vivo* likely contributes to arterial hypoxemia without major lung tissue hypoxia *per se*. However, IH could contribute to altered lipid metabolism, which may contribute to the SREBP2-mediated induction of miR-210 in ECs.

Although HIF1α has been reported to transactivate miR-210 (24, 46), we showed that SREBP2 acted as a principal transcription factor inducing miR-210 in cultured ECs responding to hypoxia (0.9% O_2) and in mouse lung under IH. Canonically, the hypoxia-induced HIF1α activates vascular endothelial growth factor, which also increases SREBP in ECs (47). In EC culture, OSA combined with PX-478, a HIF-α inhibitor, drastically decreased miR-210 concentrations in ECs (*see* Figure E3). Thus, HIF1α inductionof miR-210 is mediated by direct

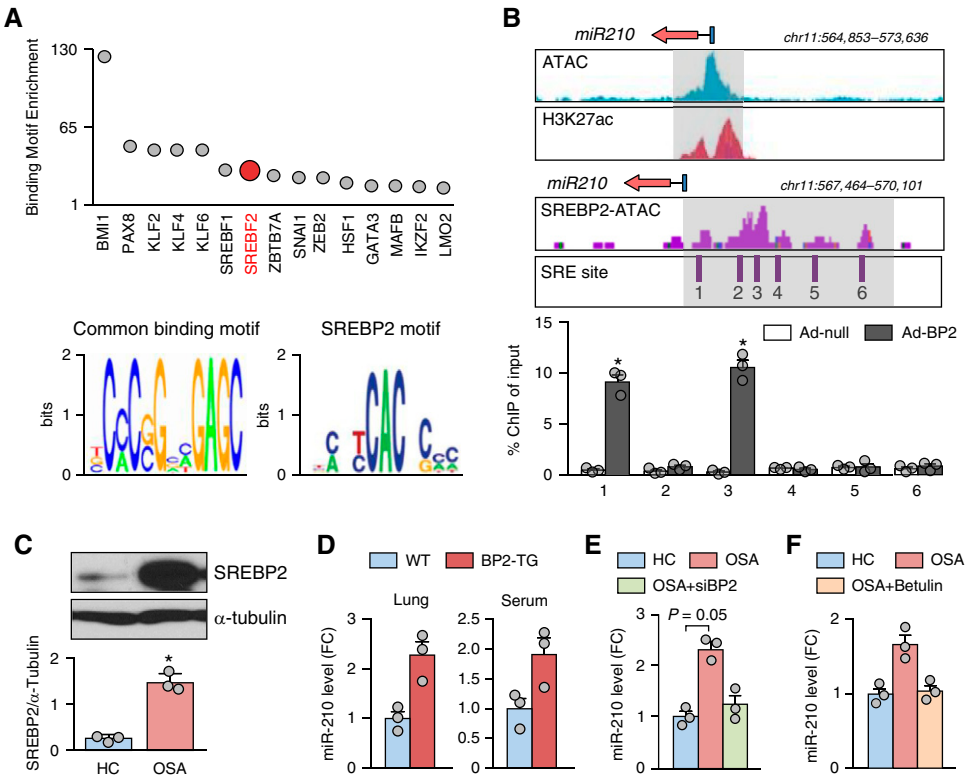

Figure 5. SREBP2 (sterol regulatory element–binding protein 2) transactivates miR-210 in ECs. (*A*) The putative transcription factors binding to the microRNA 210 (miR-210) promoter were predicted using TRANSFAC; transcription factors are listed in order of binding scores. The sequences of common binding motifs in the miR-210 active promoter and SREBP2 binding motif were deduced. (*B*) Epigenetic landscapes of assay for transposase-accessible chromatin (ATAC) signals (light blue) and H3K27ac (acetylated lysine 27 of histone H3) enrichment (red) in the promoter region of miR-210 in human umbilical vein endothelial cells (HUVECs); the highlighted region was defined as miR-210 active promoter according to these epigenetic landscapes. Putative sterol regulatory elements (SREs) and SREBP2 overexpression-induced ATAC signals (purple) in the miR-210 promoter are shown. HUVECs were infected with Ad-null or Ad-SREBP2 for 24 hours. SREBP2 binding to the miR-210 promoter was detected by SREBP2 chromatin immunoprecipitation (ChIP) followed by ChIP-quantitative PCR (qPCR). The qPCR primers are depicted by number of SRE sites. (*C*) HUVECs were treated with 10% pooled OSA or HC serum for 24 hours. SREBP2 protein concentration was detected using western blot with α-tubulin as a loading control. (*D*) RNA was isolated from lung and serum from EC-specific SREBP2-overexpression transgenic mice and their sex- and age-matched WT littermates. (*E* and *F*) HUVECs were transfected with si-SREBP2 (*E*) or treated with betulin (0.2 mg/ml; *F*) for 24 hours, followed by incubation with 10% OSA or HC serum for an additional 24 hours. In *D*–*F*, miR-210 concentration was detected using qPCR. Data are shown as mean ± SEM from at least three independent experiments. Statistical significance was determined using the Kruskal-Wallis test with Dunn's multiple comparisons or the two-tailed Mann-Whitney *U* test. $^*P < 0.05$ compared with control or between indicated groups. Ad = adenovirus; BMI1 = BMI1 proto-oncogene, polycomb ring finger; BP2-Tg = endothelial cell–specific SREBP2-overexpression transgenic mice; EC = endothelial cell; FC = fold change; GATA3 = GATA binding protein 3; HSF1 = heat shock transcription factor 1; IKZF2 = IKAROS family zinc finger 2; KLF = KLF transcription factor; LMO2 = LIM domain only 2; MAFB = MAF BZIP transcription factor B; PAX8 = paired box 8; SNAI1 = Snail family transcriptional repressor 1; SREBPF = sterol regulatory element–binding transcription factor; TF = transcription factor; WT = wild-type; ZBTB7A = zinc finger and BTB domain containing 7A; ZEB2 = zinc finger E-box binding homeobox 2.

transactivation and/or the HIF1α–vascular endothelial growth factor–SREBP2 axis.

We speculate that the OSA serum–induced miR-210 in ECs could be due to either EC uptake of miR-210 from OSA serum or a direct OSA induction of SREBP2 in ECs. Regarding possible mechanisms by which OSA serum upregulates EC SREBP2, it is likely that the OSA-associated cyclic hypoxia directly activates the SREBP2–miR-210 axis in ECs, given that hypoxia can activate SREBP2 via HIF1α (48). In addition, SREBP2 in ECs can be activated by inflammatory factors in the circulation.

Betulin has beneficial effects in tissue types including the liver (49), pancreas (50) and lung (51). Moreover, betulin may activate Lipin1/2 (52) or AMP-activated protein kinase (53) or decrease reactive oxygen species signaling (54). Thus, although data in Figures 4D, 4E, 5F, 6B, and 6D indicate its beneficial effect on EC mitochondrial function, betulin may have additional effects in tissues other than vascular endothelium via non–SREBP2-related events.

A previous study by Zhao and colleagues (36) showed that systemic hypoxia induced miR-210 in mouse bone marrow, which affects pulmonary ECs via endocrine delivery. Virga and colleagues showed that miR-210 in monocyte/myeloid lineage cells may be a source of generalized and local vascular inflammation (55). These studies

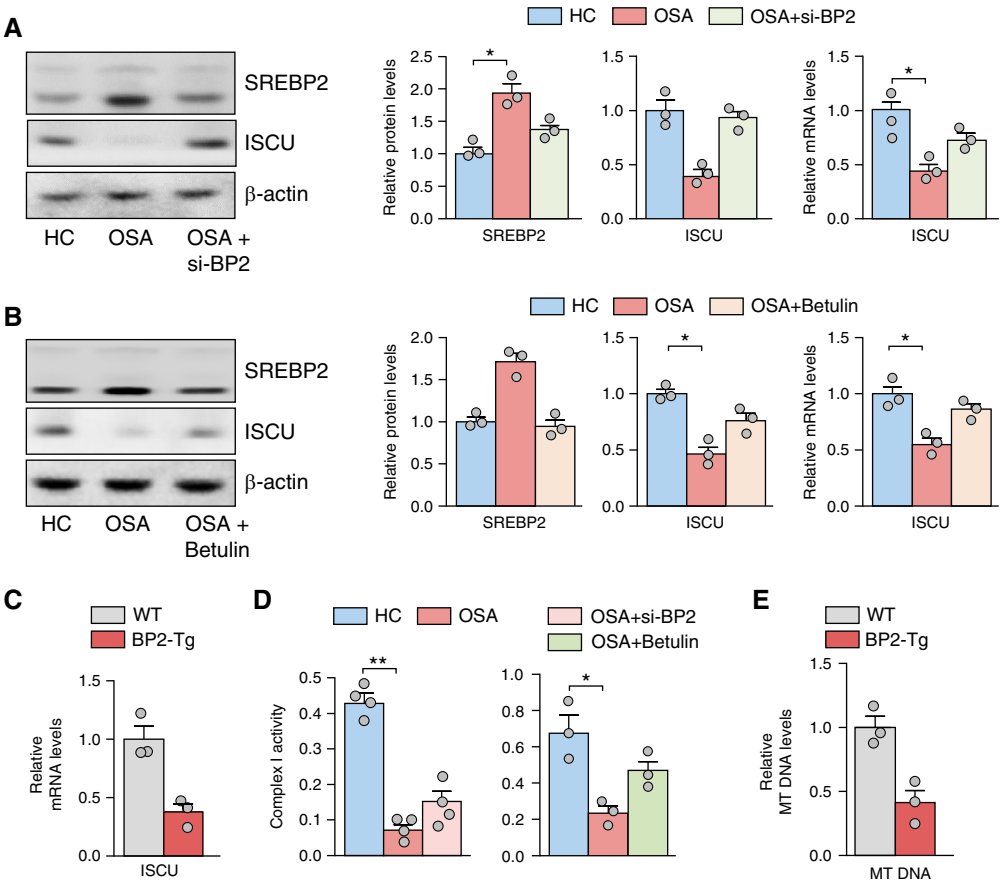

Figure 6. Obstructive sleep apnea (OSA) serum decreases iron–sulfur cluster assembly enzyme (ISCU) via SREBP2 (sterol regulatory element–binding protein 2) induction of microRNA 210 (miR-210) in endothelial cells (ECs). (*A*, *B*, and *D*) Human umbilical vein ECs were transfected with SREBP2 siRNA (si-BP2) or pretreated with betulin (0.2 mg/ml) for 24 hours, then HC or OSA serum for another 24 hours. (*C* and *E*) ECs were isolated from aorta of EC-specific SREBP2-overexpression transgenic mice (three males and three females) and their WT littermates (three males and three females). Protein concentrations of SREBP2, ISCU, and β-actin (loading control) were detected using western blot analysis (*A* and *B*). SREBP2 and ISCU mRNA concentrations were detected using quantitative PCR with β-actin as an internal control (*A*–*C*). Mitochondrial respiratory complex I activity was evaluated using enzyme activity assay (*D*). Data are shown as mean ± SEM from at least three independent experiments. Statistical significance was determined using the Kruskal-Wallis test with Dunn's multiple comparisons or the two-tailed Mann-Whitney *U* test. **P* < 0.05 compared with control or between two indicated groups. BP2-Tg = endothelial cell–specific SREBP2-overexpression transgenic; HC = healthy control; MT DNA = mitochondrial DNA; WT = wild-type.

indicate that miR-210 induction in monocytes and delivery to diverse cell types may be implicated in OSA pathophysiology. In our study, circulatory miR-210 concentration in mice under IH was associated with CD31-enriched exosomes (Figure 7), so these miRNAs originated from vascular endothelium. Despite the discrepant tissue sources where miR-210 is produced in OSA, Zhao and colleagues and our group both observed elevated miR-210 concentrations in circulation. Thus, it is plausible that distinct vascular beds may increase their uptake of exosomes enriched in miR-210. Studies of OSA have shown differential effects of the disease on various vascular beds. We have reported local differences in gene expression from mouse aorta versus human dermal biopsies versus human coronary artery ECs, which emphasizes the complexity of the underlying mechanisms (56). Conceptually, patients with OSA are at increased risk of cerebrovascular events and myocardial infarction, more so than pulmonary hypertension. Indeed, pulmonary artery ECs may be less susceptible to the effect of IH than ECs in other organ systems. To date, OSA lacks useful biomarkers that have sensitivity and specificity for OSA disease, prognostic value for important complications, and responsiveness to therapeutic interventions and that are mechanistically involved in causal pathways. Although miR-210 does not yet meet all these characteristics, serum concentration of miR-210 indeed was positively correlated with AHI in all individuals with OSA (Figure 1F). Whether miR-210 can serve as an OSA biomarker deserves further study. As well, miR-210 may be considered a therapeutic target for mitigation of OSA-induced endothelial dysfunction. Although current therapies for OSA rely on the use of continuous positive airway pressure, there are no medications addressing these comorbidities caused by OSA-induced endothelial dysfunction. Data illustrated in this study indicate that the SREBP2–miR-210 axis is involved in OSA-mediated EC dysfunction. Thus, inhibition of SREBP2 or

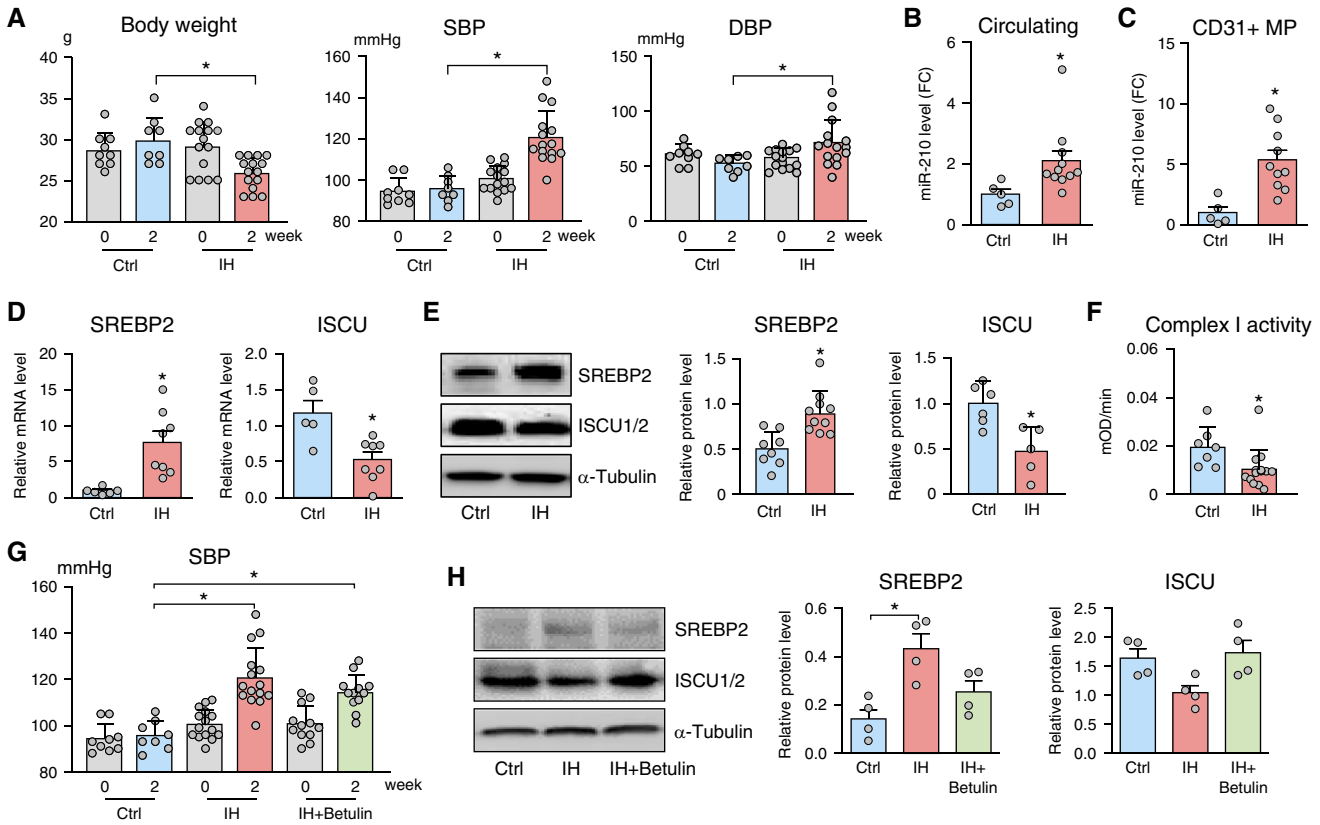

Figure 7. SREBP2 (sterol regulatory element–binding protein 2)–microRNA 210 (miR-210) impairs mitochondrial function in mice exposed to intermittent hypoxia (IH). (*A–G*) Eight-week-old C57Bl/6j mice were exposed to normoxia (21% O_2; control [Ctrl], $n = 10$ male mice) or IH (cycles of 60 s 21% O_2 + 30 s 10% O_2 for 8 h/d), with ($n = 12$ males) or without ($n = 15$ males) betulin. (*A* and *G*) Body weight, SBP, and DBP were assessed before and 2 weeks after IH treatment or under normoxia. The concentrations of miR-210 in circulation (*B*) and in $CD31^+$ MPs (*C*) were quantified using quantitative PCR. *Caenorhabditis elegans* microRNA 39 was used as a spike-in control. SREBP2 and ISCU1/2 (iron–sulfur cluster assembly enzyme 1/2) mRNA concentration (*D*) or protein concentrations (*E* and *H*) in mice aortas were quantified using quantitative PCR or western blot, respectively. (*F*) Lung tissues were extracted from mice, and mitochondrial respiratory complex I activity was assessed. Data are shown as mean ± SEM. Statistical significance was determined using one-way ANOVA followed by the Bonferroni *post hoc* test or two-tailed Student's *t* test (for parametric data). Statistical significance of nonparametric data was determined using the Kruskal-Wallis test with Dunn's multiple comparisons or the two-tailed Mann-Whitney *U* test. $^*P < 0.05$ between indicated groups. CD31 = cluster of differentiation 31; DBP = diastolic blood pressure; FC = fold change; MP = microparticles; SBP = systolic blood pressure.

miR-210 via administration of SREBP2 inhibitors or miR-210–neutralizing antagomirs may be promising therapeutic avenues for mitigation of comorbidities resulting from OSA-induced endothelial dysfunction.

Despite our study's strengths, we acknowledge several limitations. First, we did not have interventional data from humans after continuous positive airway pressure therapy, for example. Thus, our human findings are primarily cross-sectional, although we view the findings as robust given that they were reproducible from two independent sources. We did not measure EC mitochondrial dysfunction in humans. Such measurements are notoriously challenging, but we consider that our *in vivo* mouse studies and our *in vitro* observations are rigorous and robust. Third, our sample size could be considered modest. However, we are hopeful that our novel findings will encourage more rigorous research. Despite these limitations, we consider our new findings worthy of further pursuit.

Conclusions

Using *in vitro*, *in vivo*, and human data, we have demonstrated a potentially major role of miR-210 in mediating OSA-induced vascular risk. The mechanisms underlying OSA risk may be modulated by SREBP2–miR-210–induced mitochondrial dysfunction in ECs. The findings provide compelling evidence that miR-210 may be a suitable candidate as an OSA biomarker and a therapeutic target for subsequent interventional studies. Only through rigorous multidisciplinary research are new therapeutic approaches for OSA likely to emerge. ■

Author disclosures are available with the text of this article at www.atsjournals.org.

Acknowledgment: The authors thank Dr. Jian Kang (University of California, San Diego), Yuqing Zhang (University of California, San Diego), Yuning Wang (Salk Institute), and Baochang Lai (Xi'an Jiaotong University) for their technical assistance.

References

1. Resta O, Foschino Barbaro MP, Bonfitto P, Talamo S, Mastrosimone V, Stefano A, *et al.* Hypercapnia in obstructive sleep apnoea syndrome. *Neth J Med* 2000;56:215–222.
2. Owens RL, Eckert DJ, Yeh SY, Malhotra A. Upper airway function in the pathogenesis of obstructive sleep apnea: a review of the current literature. *Curr Opin Pulm Med* 2008;14:519–524.
3. Dewan NA, Nieto FJ, Somers VK. Intermittent hypoxemia and OSA: implications for comorbidities. *Chest* 2015;147:266–274.
4. Bisogni V, Pengo MF, Maiolino G, Rossi GP. The sympathetic nervous system and catecholamines metabolism in obstructive sleep apnoea. *J Thorac Dis* 2016;8:243–254.
5. Hoffstein V, Szalai JP. Predictive value of clinical features in diagnosing obstructive sleep apnea. *Sleep* 1993;16:118–122.
6. Lattimore JD, Celermajer DS, Wilcox I. Obstructive sleep apnea and cardiovascular disease. *J Am Coll Cardiol* 2003;41:1429–1437.
7. Devulapally K, Pongonis R Jr, Khayat R. OSA: the new cardiovascular disease: part II. Overview of cardiovascular diseases associated with obstructive sleep apnea. *Heart Fail Rev* 2009;14:155–164.
8. Javaheri S, Barbe F, Campos-Rodriguez F, Dempsey JA, Khayat R, Javaheri S, *et al.* Sleep apnea: types, mechanisms, and clinical cardiovascular consequences. *J Am Coll Cardiol* 2017;69:841–858.
9. Atkeson A, Jelic S. Mechanisms of endothelial dysfunction in obstructive sleep apnea. *Vasc Health Risk Manag* 2008;4:1327–1335.
10. Feng J, Zhang D, Chen B. Endothelial mechanisms of endothelial dysfunction in patients with obstructive sleep apnea. *Sleep Breath* 2012;16:283–294.
11. Lavie L. Oxidative stress inflammation and endothelial dysfunction in obstructive sleep apnea. *Front Biosci (Elite Ed)* 2012;4:1391–1403.
12. Campillo N, Falcones B, Montserrat JM, Gozal D, Obeso A, Gallego-Martin T, *et al.* Frequency and magnitude of intermittent hypoxia modulate endothelial wound healing in a cell culture model of sleep apnea. *J Appl Physiol (1985)* 2017;123:1047–1054.
13. Atkeson A, Yeh SY, Malhotra A, Jelic S. Endothelial function in obstructive sleep apnea. *Prog Cardiovasc Dis* 2009;51:351–362.
14. Bartel DP. Metazoan microRNAs. *Cell* 2018;173:20–51.
15. Li K, Chen Z, Qin Y, Wei Y. MiR-664a-3p expression in patients with obstructive sleep apnea: a potential marker of atherosclerosis. *Medicine (Baltimore)* 2018;97:e9813.
16. Freitas LS, Silveira AC, Martins FC, Costa-Hong V, Lebkuchen A, Cardozo KHM, *et al.* Severe obstructive sleep apnea is associated with circulating microRNAs related to heart failure, myocardial ischemia, and cancer proliferation. *Sleep Breath* 2020;24:1463–1472.
17. Gongol B, Shang F, He M, Zhao Y, Shi W, Cheng M, *et al.* Serum miR-92a is elevated in children and adults with obstructive sleep apnea. *J Mol Biomark Diagn* 2020;11:11.
18. Huang X, Ding L, Bennewith KL, Tong RT, Welford SM, Ang KK, *et al.* Hypoxia-inducible miR-210 regulates normoxic gene expression involved in tumor initiation. *Mol Cell* 2009;35:856–867.
19. Lacedonia D, Scioscia G, Pia Palladino G, Gallo C, Carpagnano GE, Sabato R, *et al.* MicroRNA expression profile during different conditions of hypoxia. *Oncotarget* 2018;9:35114–35122.
20. Chen Z, Li Y, Zhang H, Huang P, Luthra R. Hypoxia-regulated microRNA-210 modulates mitochondrial function and decreases ISCU and COX10 expression. *Oncogene* 2010;29:4362–4368.
21. Devlin C, Greco S, Martelli F, Ivan M. miR-210: more than a silent player in hypoxia. *IUBMB Life* 2011;63:94–100.
22. Nakada C, Hijiya N, Tsukamoto Y, Yano S, Kai T, Uchida T, *et al.* A transgenic mouse expressing miR-210 in proximal tubule cells shows mitochondrial alteration: possible association of miR-210 with a shift in energy metabolism. *J Pathol* 2020;251:12–25.
23. Doughan AK, Harrison DG, Dikalov SI. Molecular mechanisms of angiotensin II-mediated mitochondrial dysfunction: linking mitochondrial oxidative damage and vascular endothelial dysfunction. *Circ Res* 2008; 102:488–496.
24. Chan SY, Zhang YY, Hemann C, Mahoney CE, Zweier JL, Loscalzo J. MicroRNA-210 controls mitochondrial metabolism during hypoxia by repressing the iron–sulfur cluster assembly proteins ISCU1/2. *Cell Metab* 2009;10:273–284.
25. Kluge MA, Fetterman JL, Vita JA. Mitochondria and endothelial function. *Circ Res* 2013;112:1171–1188.
26. Tong WH, Rouault TA. Functions of mitochondrial ISCU and cytosolic ISCU in mammalian iron–sulfur cluster biogenesis and iron homeostasis. *Cell Metab* 2006;3:199–210.
27. Favaro E, Ramachandran A, McCormick R, Gee H, Blancher C, Crosby M, *et al.* MicroRNA-210 regulates mitochondrial free radical response to hypoxia and krebs cycle in cancer cells by targeting iron sulfur cluster protein ISCU. *PLoS One* 2010;5:e10345.
28. Li H, Liu Y, Shang L, Cai J, Wu J, Zhang W, *et al.* Iron regulatory protein 2 modulates the switch from aerobic glycolysis to oxidative phosphorylation in mouse embryonic fibroblasts. *Proc Natl Acad Sci U S A* 2019;116:9871–9876.
29. White K, Lu Y, Annis S, Hale AE, Chau BN, Dahlman JE, *et al.* Genetic and hypoxic alterations of the microRNA-210-ISCU1/2 axis promote iron-sulfur deficiency and pulmonary hypertension. *EMBO Mol Med* 2015;7:695–713.
30. Brown MS, Goldstein JL. The SREBP pathway: regulation of cholesterol metabolism by proteolysis of a membrane-bound transcription factor. *Cell* 1997;89:331–340.
31. Xiao H, Lu M, Lin TY, Chen Z, Chen G, Wang WC, *et al.* Sterol regulatory element binding protein 2 activation of NLRP3 inflammasome in endothelium mediates hemodynamic-induced atherosclerosis susceptibility. *Circulation* 2013;128:632–642.
32. Chen Z, Wen L, Martin M, Hsu CY, Fang L, Lin FM, *et al.* Oxidative stress activates endothelial innate immunity via sterol regulatory element binding protein 2 (SREBP2) transactivation of microRNA-92a. *Circulation* 2015;131:805–814.
33. Guo C, Chi Z, Jiang D, Xu T, Yu W, Wang Z, *et al.* Cholesterol homeostatic regulator scap-srebp2 integrates nlrp3 inflammasome activation and cholesterol biosynthetic signaling in macrophages. *Immunity* 2018;49:842–856.e7.
34. Livak KJ, Schmittgen TD. Analysis of relative gene expression data using real-time quantitative PCR and the 2(-delta delta C(T)) method. *Methods* 2001;25:402–408.
35. Kochan-Jamrozy K, Króliczewski J, Moszyńska A, Collawn JF, Bartoszewski R. miRNA networks modulate human endothelial cell adaptation to cyclic hypoxia. *Cell Signal* 2019;54:150–160.
36. Zhao J, Florentin J, Tai YY, Torrino S, Ohayon L, Brzoska T, *et al.* Long range endocrine delivery of circulating miR-210 to endothelium promotes pulmonary hypertension. *Circ Res* 2020;127:677–692.
37. Kusnadi A, Park SH, Yuan R, Pannellini T, Giannopoulou E, Oliver D, *et al.* The cytokine TNF promotes transcription factor SREBP activity and binding to inflammatory genes to activate macrophages and limit tissue repair. *Immunity* 2019;51:241–257.e9.
38. Chen C, Khismatullin DB. Oxidized low-density lipoprotein contributes to atherogenesis via co-activation of macrophages and mast cells. *PLoS One* 2015;10:e0123088.
39. Dematteis M, Julien C, Guillermet C, Sturm N, Lantuejoul S, Mallaret M, *et al.* Intermittent hypoxia induces early functional cardiovascular remodeling in mice. *Am J Respir Crit Care Med* 2008;177:227–235.
40. Zamarron C, García Paz V, Riveiro A. Obstructive sleep apnea syndrome is a systemic disease: current evidence. *Eur J Intern Med* 2008;19: 390–398.
41. Butt M, Dwivedi G, Khair O, Lip GY. Obstructive sleep apnea and cardiovascular disease. *Int J Cardiol* 2010;139:7–16.
42. Kohler M, Stradling JR. Mechanisms of vascular damage in obstructive sleep apnea. *Nat Rev Cardiol* 2010;7:677–685.
43. Cardenas-Rodriguez M, Chatzi A, Tokatlidis K. Iron–sulfur clusters: from metals through mitochondria biogenesis to disease. *J Biol Inorg Chem* 2018;23:509–520.
44. Qin Q, Furong W, Baosheng L. Multiple functions of hypoxia-regulated miR-210 in cancer. *J Exp Clin Cancer Res* 2014;33:50.
45. Bodempudi V, Hergert P, Smith K, Xia H, Herrera J, Peterson M, *et al.* miR-210 promotes IPF fibroblast proliferation in response to hypoxia. *Am J Physiol Lung Cell Mol Physiol* 2014;307:L283–L294.
46. Karshovska E, Wei Y, Subramanian P, Mohibullah R, Geißler C, Baatsch I, *et al.* Hif-1alpha (hypoxia-inducible factor-1alpha) promotes macrophage necroptosis by regulating miR-210 and miR-383. *Arterioscler Thromb Vasc Biol* 2020;40:583–596.

47. Zhou RH, Yao M, Lee TS, Zhu Y, Martins-Green M, Shyy JY. Vascular endothelial growth factor activation of sterol regulatory element binding protein: a potential role in angiogenesis. *Circ Res* 2004;95:471–478.
48. Zhu J, Jiang X, Chehab FF. FoxO4 interacts with the sterol regulatory factor SREBP2 and the hypoxia inducible factor HIF2α at the CYP51 promoter. *J Lipid Res* 2014;55:431–442.
49. Buko V, Kuzmitskaya I, Kirko S, Belonovskaya E, Naruta E, Lukivskaya O, *et al.* Betulin attenuated liver damage by prevention of hepatic mitochondrial dysfunction in rats with alcoholic steatohepatitis. *Physiol Int* 2019;106:323–334.
50. Zhou Z, Choi JW, Shin JY, Kim DU, Kweon B, Oh H, *et al.* Betulinic acid ameliorates the severity of acute pancreatitis via inhibition of the NF-κB signaling pathway in mice. *Int J Mol Sci* 2021; 22:6871.
51. Yue Q, Deng X, Li Y, Zhang Y. Effects of betulinic acid derivative on lung inflammation in a mouse model of chronic obstructive pulmonary disease induced by particulate matter 2.5. *Med Sci Monit* 2021;27: e928954.
52. Dou JY, Jiang YC, Hu ZH, Yao KC, Yuan MH, Bao XX, *et al.* Betulin targets lipin1/2-mediated p2 × 7 receptor as a therapeutic approach to attenuate lipid accumulation and metaflammation. *Biomol Ther (Seoul)* 2022;30:246–256.
53. Ci X, Zhou J, Lv H, Yu Q, Peng L, Hua S. Betulin exhibits anti-inflammatory activity in LPS-stimulated macrophages and endotoxin-shocked mice through an AMPK/AKT/Nrf2-dependent mechanism. *Cell Death Dis* 2017;8:e2798.
54. Fu JY, Qian LB, Zhu LG, Liang HT, Tan YN, Lu HT, *et al.* Betulinic acid ameliorates endothelium-dependent relaxation in L-NAME-induced hypertensive rats by reducing oxidative stress. *Eur J Pharm Sci* 2011; 44:385–391.
55. Virga F, Cappellesso F, Stijlemans B, Henze AT, Trotta R, Van Audenaerde J, *et al.* Macrophage miR-210 induction and metabolic reprogramming in response to pathogen interaction boost life-threatening inflammation. *Sci Adv* 2021;7:eabf0466.
56. Kaczmarek E, Bakker JP, Clarke DN, Csizmadia E, Kocher O, Veves A, *et al.* Molecular biomarkers of vascular dysfunction in obstructive sleep apnea. *PLoS One* 2013;8:e70559.